THE ASTROPHYSICAL JOURNAL, 296:458–460, 1985 September 15

STRONG SOURCE VLBI OBSERVATIONS AT 22 GHz

C. R. LAWRENCE,[1] A. C. S. READHEAD,[1] R. P. LINFIELD,[2] D. G. PAYNE,[2] R. A. PRESTON,[2]
R. T. SCHILIZZI,[3] R. W. PORCAS,[4] R. S. BOOTH,[5] AND B. F. BURKE[6]

Received 1985 January 14; accepted 1985 March 18

ABSTRACT

Twenty-six strong high-frequency radio sources have been observed at 22.3 GHz on interferometer baselines of $\sim 5 \times 10^8$ wavelengths. Twenty-five were detected, and 14 have mean visibilities over 50%. The strongest sources as a group are more heavily resolved than the weaker sources.

Subject headings: interferometry — radio sources: general

I. INTRODUCTION

Over the last few years, very long baseline interferometer maps have been made of many active galactic nuclei at a resolution of ~ 1 mas. These maps often have unresolved features, suggesting that maps at even higher resolution are needed. Without going into space, this can be accomplished only by increasing the observing frequency. Accordingly, 22 GHz is now a standard observing frequency in the US and European VLBI networks. With intercontinental baselines, maps can be made at this frequency with ~ 0.4 mas resolution.

Although 22 GHz is now a network standard, relatively few continuum studies have been made at this frequency. There are two reasons for this. First, there are still relatively few antennas that can observe at 22 GHz, and antenna and receiver performance are, in general, not as good as at lower frequencies. Second, in most of the sources that have been observed, only a small fraction of the total flux density comes from the smallest components (e.g., 3C 84; Readhead *et al.* 1983). These sources are among the strongest in the sky at high frequencies. If weaker sources were similarly resolved at 22 GHz, there would be few sources that could be mapped, given the sensitivity limits of existing antennas.

To determine the sub–milliarcsecond structure of a reasonable sample of sources, and in particular to see whether weaker sources are as heavily resolved as the strongest sources, we have begun a study of 50 moderately strong high-frequency sources. The observations described in this paper are the first part of that work, and were designed to give UV sampling adequate for simple model fitting, if not for mapping. Even at this stage, it is already clear that strong sub–milliarcsecond structure is common in this class of source.

II. SOURCE SELECTION AND OBSERVATIONS

Twenty-six sources were observed in 1984 January. Twenty were taken from the lists of Owen, Spangler, and Cotton (1980) or Geldzahler and Kühr (1983), with $S(31.4 \text{ GHz}) \geq 1.5$ Jy. All but three had $\alpha(31.4, 90) < +0.5$ ($S \propto \nu^{-\alpha}$). The other six sources, with $0.47 \text{ Jy} \leq S(22) \leq 3.0$ Jy, were from the 6 cm survey of Pearson and Readhead (1984), with "compact" or "very compact" structure. Our aim in selecting the sources was to maximize the probability of compact structure, so in general we chose the strongest flat-spectrum sources that could be scheduled efficiently. Some of the sources had been previously mapped at 22 GHz, but were included either to aid in fringe searching, or as controls.

Each source was observed for 5 or 10 minutes at three or four hour angles. The Mk II recording system, with a bandwidth of 2 MHz, was used. Six stations were scheduled: Onsala (26 m), Effelsberg (Eff; 100 m), Haystack (37 m), Green Bank (43 m), one VLA antenna (25 m), and Owens Valley (OVRO; 40 m). Meteorological and technical difficulties at Haystack, Green Bank, and the VLA left only three antennas for more than half of the observations. Following correlation, the data were coherently averaged over 2 minute intervals, the coherence time for these observations.

III. RESULTS

All but one source was detected on the Eff–OVRO baseline ($D > 5 \times 10^8$ wavelengths). Figure 1 shows the distribution of mean Eff–OVRO visibilities. Table 1 gives the total flux density, the mean Eff–OVRO correlated flux density, and $\bar{\Gamma}$, the mean fractional correlated flux density or mean visibility, for the sources. Fourteen sources have mean visibilities over 50%. The strongest, best-known sources are clustered at the low end of the figure. This can also be seen in Table 1, where

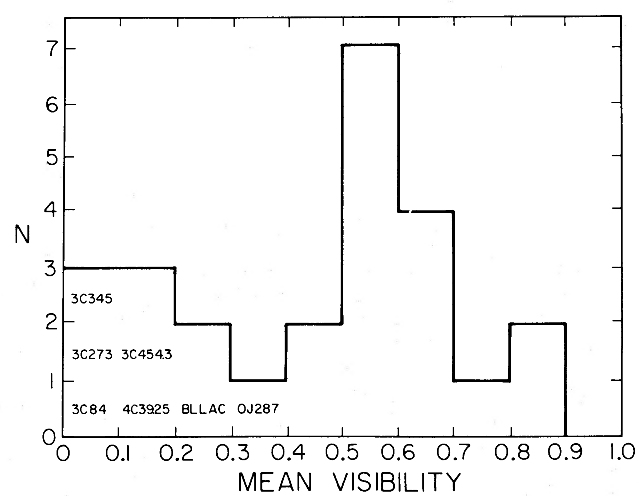

FIG. 1.—Distribution of mean visibilities on the $\sim 5 \times 10^8$ wavelength Eff–OVRO baseline.

[1] California Institute of Technology.
[2] Jet Propulsion Laboratory.
[3] Radiosterrenwacht Dwingeloo.
[4] Max-Plank-Institut für Radioastronomie.
[5] Onsala Space Observatory.
[6] Department of Physics, Massachusetts Institute of Technology.

TABLE 1

FLUX DENSITIES AND MEAN VISIBILITIES OF SOURCES

Source	Optical Identification[a]	Total Flux Density (Jy)	Correlated Flux Density Eff–OVRO (Jy)	$\bar{\Gamma}$
0007+106 (III Zw 2)	Q	1.2	0.88	0.71
0016+731	Q	1.2	0.63	0.50
0133+476	Q	2.8	2.4	0.85
0224+671	Q	1.8	1.1	0.65
0234+285	Q	3.1	1.7	0.54
0235+164	B	1.5	0.71	0.47
0300+471	B	2.3	1.1	0.60
3C 84	G	50.	1.2	0.02
0355+508 (NRAO 150)	E	7.0	3.5	0.50
0454+844	Q	0.47	...	...
0716+714	Q	1.1	0.56	0.51
0804+499	Q	0.65	0.53	0.82
0851+202 (OJ 287)	B	7.0	2.4	0.34
0859+470	Q	0.57	0.26	0.46
0923+392 (4C 39.25)	Q	2.7	0.35	0.13
3C 273	Q	44.	...[b]	...
1308+326	B	3.1	2.1	0.68
1633+382	Q	2.6	0.62	0.24
1637+575	Q	1.6	0.94	0.59
3C 345	Q	14.	1.3	0.09
1642+690	Q	1.2	0.67	0.56
1739+522	Q	3.0	2.0	0.65
1803+784	G	2.7	1.4	0.53
2005+403	Q	3.3	0.50	0.15
BL Lac	B	2.8	0.59	0.21
3C 454.3	Q	5.5	0.77	0.14

[a] Q—QSO; B—BL Lac; G—Galaxy; E—Empty field.

[b] The 3C 273 data could not be calibrated on this baseline, but the source was easily detected.

the sources span a range of almost 90 in total flux density, but less than 15 in correlated flux density. The flux densities are subject to substantial errors, perhaps 20% or 30% in some cases, due to the difficulties of calibrating sparse data taken during bad weather. The mean visibilities, however, should be more reliable, since the calibration errors affect both the total and correlated flux densities in the same way, and divide out in the ratio.

Closure amplitudes, usually at three hour angles, are available for eight sources, and allow us to estimate their angular sizes. In seven cases, we compared closure amplitudes calculated for a single circular Gaussian brightness distribution with the observations. In the case of 0234+285 we had enough closure amplitudes to justify trying a noncircular Gaussian distribution. The sizes that gave the best agreement are listed in Table 2, along with the corresponding brightness temperatures. The ranges give a conservative judgment of how large or small the model component can be without clear disagreement with the data. We emphasize that these estimates are model dependent. Nevertheless, the agreement between a given model and the measured closure amplitudes is quite sensitive to angular size.

The angular size of 3C 84 given in Table 2 is consistent with the size of the most compact component in the map of Readhead *et al.* (1983); however, if their map is used as a source model, the resulting closure amplitudes are clearly inconsistent with our new data. The most likely explanation for this is that the structure of 3C 84 has changed over the last 2 yr. Although the total flux density of the source has not changed appreciably during that time, so little of the total flux density comes from

TABLE 2

ANGULAR SIZES AND BRIGHTNESS TEMPERATURES OF SOURCES

Source	z	Angular Size (mas)	T_B[a] (10^{12} K)
0007+106	0.089	$0.00^{+0.15}$	>0.11
0133+476	0.860	0.08 ± 0.08	1.7
0234+285	1.207	$0.3 \pm 0.2 \times 0.03^{+0.09}_{-0.03}$, P.A. = $-5°^{+15°}_{-25°}$	1.3
0300+471	...	$0.11^{+0.05}_{-0.11}$	0.4
3C 84	0.018	0.31 ± 0.10	0.04
0355+508	...	$0.15^{+0.05}_{-0.10}$	0.8
0851+202	0.306	0.21 ± 0.10	0.2
3C 454.3	0.859	0.20 ± 0.10	0.09

[a] Peak brightness temperature of the Gaussian models (for 0234, $\theta_{FWHM} = 0.09$ was used). The Eff–OVRO correlated flux density was used, corrected for resolution as calculated from the model. Unknown redshifts were assumed to be unity.

the most compact component that even large changes in it have little effect on the total. Only a new map of 3C 84 can confirm changes in structure. Nevertheless, this source serves as a useful reminder that it is always risky to reduce a potentially complicated structure to a single number on the basis of sketchy data. The numbers in Table 2 should be treated with caution.

From Table 1 and Figure 1 it is clear that the fainter sources have a larger fraction of unresolved flux density than the stronger sources. One might expect this to be a distance selection effect, but the factor of 40 between the extreme brightness temperatures in Table 2 argues against this. There seems to be no easy way to make standard radio candles out of the sources.

It is interesting to note that only a few of the sources we have observed appear to be unresolved, although many of them are unresolved at longer wavelengths. The sizes in Table 2 should be compared with the ~ 0.4 mas beam usually achieved in 22 GHz mapping experiments. It is clear that many sources have structure that can be mapped with baselines of 5×10^8 wavelengths or longer.

IV. SUMMARY

We have detected 25 out of 26 high-frequency radio sources on baselines of $\sim 5 \times 10^8$ wavelengths. Fourteen have mean visibilities on the Eff–OVRO baseline greater than 50%. Crude angular sizes have been calculated for eight sources using closure amplitudes. These results are the best observational evidence that 22 GHz VLBI is an essential tool in the study of active nuclei. The sources are in many cases largely unresolved, implying that a combination of ground-based observations at even higher frequencies and observations with orbiting antennas will be required in the future.

REFERENCES

Geldzahler, B. J., and Kühr, H. 1983, *A.J.*, **88**, 1126.
Owen, F. N., Spangler, S. R., and Cotton, W. D. 1980, *A.J.*, **85**, 351.
Pearson, T. J., and Readhead, A. C. S. 1984, in *IAU Symposium 110, VLBI and Compact Radio Sources*, ed. R. Fanti, K. Kellermann, and G. Setti (Dordrecht: Reidel), p. 15.
Readhead, A. C. S., Hough, D. H., Ewing, M. S., Walker, R. C., and Romney, J. D. 1983, *Ap. J.*, **265**, 107.
Readhead, A. C. S., Walker, R. C., Pearson, T. J., and Cohen, M. H. 1980, *Nature*, **285**, 137.
Readhead, A. C. S., and Wilkinson, P. N. 1978, *Ap. J.*, **223**, 25.

R. S. Booth: Onsala Space Observatory, S-430 34 Onsala, Sweden

B. F. Burke: Department of Physics, Massachusetts Institute of Technology, Cambridge, MA 02139

C. R. Lawrence and A. C. S. Readhead: Owens Valley Radio Observatory, 105-24, California Institute of Technology, Pasadena, CA 91125

R. P. Linfield, D. G. Payne, and R. A. Preston: 264-781 Jet Propulsion Laboratory, Pasadena, CA 91109

R. W. Porcas: Max-Planck-Institut für Radioastronomie, Auf dem Hügel 69, D-5300, Bonn A, West Germany

R. T. Schilizzi: Radiosterrenwacht Dwingeloo, Postbus 2, 7990 AA Dwingeloo, The Netherlands